Cell Sensing of Micro- and Nano- Topography

Robert Hartley BSc (Hons)

Centre for Cell Engineering

Division of Infection and Immunity

Institute of Biomedical and Life Sciences

University of Glasgow

A Thesis Submitted to the Faculty of Biological and Life Sciences of the University of Glasgow for the Degree of Doctor of Philosophy.

June 2002

Acknowledgements

I would like to thank my supervisor Professor Adam Curtis for his support during the last four years. I would particularly like to thank him for gathering together a wonderful group of people in the laboratory. It really has been a pleasure working alongside everyone. In particular I must mention the help, encouragement and assistance of my good friend Mathis Riehle. It would also not have been as happy an experience without John Gallagher who I shared and office with for almost eighteen months. Socially, I'd like to thank Adam and in particular his wife Ann for all the parties, Mathis and Douglas Hamilton for our "monthly lab meeting" over a beer, and John Gallagher and Kate Broderick for "Friday wind-downs".

Academically I would like to voice my sincere thanks to Adam for his guidance, Mathis for help with video microscopy and data analysis, Gordon Campbell and Graham Tobasnick for technical assistance. Last but not least Scot Arkison for coming in on the odd Saturday (even though he left biology) to assist with gene expression studies.

Finally, but most importantly, I would like to dedicate this thesis to my beautiful wife Amanda. Her support and understanding will be remembered forever.

Summary

In this thesis I have assessed the reaction of endothelia and epithelia to micro and nano-topography. I specifically analysed the movement, cytoskeletal reaction and signal transduction mechanisms involved.

I have shown that irrespective of subjective morphology, the substratum topography underlying cells had the ability to affect the cytoskeletal alignment and directionality of induced movement. The reaction of the three main elements of the cytoskeleton; actin fibres, intermediate filaments and microtubules, had different basal-apical distributions and were oriented along the grooves.

Particularly significant was my description of growth factor induced, directed movement of MDCK epithelia on grooved topography. This directed movement was observed whether the cells were elongated individual cells or non-morphologically reactive multicellular monolayers. Movement was shown to flow along the grooves. This directionality may have particular relevance in the repair of lesions or situations where one requires differential positioning or migration of cell types (Babu and Wells 2001). I also assessed the possibility of unidirectional guidance using a surface with major grooves for bi-directional elongation. This particular surface* had gradients in the troughs to confer unidirectional movement.

I also show that a grooved topographical substrate, analogous to fibre dimensions encountered in-vivo, rescues inhibition of cell-spreading (by signal pathway

blockade) in the direction of the groove but not anti-parallel. The spreading was dependent on groove depth and is consistent with elongation on variable depths.

I propose a new hypothesis that bi-directional signalling mechanisms are involved in cell spreading, and elongation is by a different mechanism from lateral spreading. Recently, following this work and during the final writing of this thesis, a bi-directional spreading hypothesis has also been speculated by Levina et al (2001). In this paper only the phenotypic observation noticed by Curtis and Clark, Brunette, and Dunn was described, but with emphasis on cell width rather than elongation. I have further qualified the hypothesis by showing the lateral spreading reaction, but not elongation, is controlled by two signalling pathways, PI3-kinase and MAPK. When blocked, these inhibit the radial spreading reaction on flat surfaces.

*Made by David Baxter (BSc. Honours Student, University of Glasgow) during his final year project. I gratefully thank David for the use of this structure.

Abbreviations

ANOVA	Analysis of Variance
B10D2	Endothelial Cell Line
CCE	Centre for Cell Engineering
CNS	Central Nervous System
ECM	Extracellular Matrix
EGFP	Enhanced Green Fluorescent Protein
ERK	Extracellular Related Kinase
FA	Focal Adhesion
F-Actin	Filamentous Actin
FAK	Focal Adhesion Kinase
GAP	GTP Activating Protein
GFP	Green Fluorescent Protein
GTP	Guanine tri-Phosphate (Magnesium Complex)
HGF	Hepatocyte Growth Factor
HGTFN	Human Granuloma Tissue Cell Line
IRM	Interference reflection Microscopy
KGF	Keratinocyte Growth Factor
MAPK	Mitogen Activated Protein Kinase
MAPKK	Mitogen Activated Protein Kinase Kinase
MDCK	Maden Darby Canine Kidney Cell line
mRNA	Messenger RNA

MTOC	Microtubule Organising Centre
p388D1	Macrophage Cell Line
PCR	Polymerase Chain Reaction
PDGF	Platelet Derived Growth Factor
PKC	Protein Kinase C
PI3	Phosphatidyl Inositol 3
PLC	Phospho Lipase C
Rho	Ras Homology
STAT	Signal Transducers and Activators of Transcription

Chapter 1

Introduction: A Historical Perspective

From early on in the last century it was clear that cells would react to fibres and undergo locomotory guidance. Carrel and Burrows (Carrel and Burrows 1911) described "Spindle" cells on the fibrous part of plasma clots when describing the growth characteristics of Rous chicken sarcoma in culture. Harrison (Harrison 1911) also noticed polarisation and movement in the plane of spider web fibres. Later Paul Weiss, working on fibrin clots, termed the elongated reaction of cells to the clot and one-another as "contact guidance". He noted that, where stretch was invoked by tension in the fibrin clot, cell elongation was more pronounced (Weiss and Garber 1952). Weiss also demonstrated that, although this elongated morphology was evident in the areas with uni-axial stretch and tension, and decreased as stretch decreased, the full range of morphologies from radial to bipolar could be viewed in areas where there was little stretch. Therefore, there must be another factor to account for the range of morphologies, and in particular the elongation without stretch cue. Perhaps, in this case, the apparent elongation was due to either fibre bundling, local tension forces or topographical features in the clot itself. In the late 1950's Abercrombie, Heaysman and Karthauser (Abercrombie, Heaysman et al. 1957) assessed contact inhibition between chick and mouse fibroblasts and mouse sarcoma in co-culture of explants. They showed that the fibroblasts of different species displayed contact inhibition to each other but the effect lessened when each was cultured with sarcoma. This indicated contact inhibition was not species exclusive

and Abercrombie suggested that cancerous cells might react differently to normal cells. McCartney and Buck later confirmed this using grooved substrates (McCartney and Buck 1981). One interesting point in Abercrombie's work was that the cells were cultured on fowl plasma and embryo extract. This may have a topographic and/or chemical input giving a dual cue. Rather than speculate on a multipart system and use this as a basis for investigating "contact inhibition", it is simpler and preferable to investigate individual, influential factors, in a model system. To achieve this, the contact inhibition model-system used in the last few decades, where a topographical substrate mimics the dimensions of the clot fibres, has mainly been an array of parallel lines or grooves in a homogeneous substrate. On parallel grooves almost all cells elongate in the direction of the groove. To account for such topographic phenomenon, three main hypotheses originated from subsequent work.

Dunn and Heath (Dunn and Heath 1976) suggested that the substrate placed mechanical restrictions on the microfilaments, preventing them from forming. Using glass tubes formed by "pulling" over a bunsen, they noticed that the cells in the smaller tubes (greater curvature) were more elongated along the tube, perhaps as a consequence of not being able to spread round the increased curvature. They also used prisms, with different angles to prevent cells crossing an angled boundary, to determine the angular threshold. In these prism experiments, they noticed lamellipodia crossing the boundary but with no continuous cross-ridge microfilaments. Upon this clear observation they postulated the microfilament model in which the inability of the microfilaments to form over an angle threshold was the driving force for parallel alignment.

Ohara and Buck (1979) suggested an alternative whereby the gaps between the groove ridges reduce the area in one direction upon which, the focal contacts form simply because of their size. Therefore they are able, by default, to create more contacts in one direction. However, this "favoured" scenario does not account for the depth dependency of the work by Clarke and Curtis (Clark, Connolly et al. 1991), nor in the scenario where cells migrate from a large flat surface and meet a groove (e.g. a scratch on the surface of a flat coverslip). In addition, they suggested that filopodia were not aligned by the grooves.

In the third hypothesis, Curtis and Clark (Clark, Connolly et al. 1991) suggested that rather than the discontinuities acting as a barrier, they become sites of preferential adhesion and this determines the elongated parallel morphology. Granted this does not account for the depth dependency scenario by itself, but it does suggest a potential mechanism whereby flattening and searching lamellipodia and filopodia are able to anchor nascent adhesion sites faster in one direction. This, in turn, would preferentially nucleate subsequent fibre extension and hence directionality. The increase in adhesion formation on grooves was confirmed by Wojciak-Stothard (Wojciak-Stothard, Madeja et al. 1995) when she showed p388D1 macrophage like cells adhere faster to grooves than to a flat surface. One must bear in mind, in cross cell-type comparison, that different cell types will have different reaction profiles on grooves (Clarke, Connolly et al. 1991; Hamilton 2000). . Therefore, this faster adhesion should not be taken as definitive of all cells, especially since macrophage cells are more reactive to shallow topography than any other cell type I am aware of in the literature.

Aside from rigid topography, on which the three main hypotheses have been based, flexible substrates and cyclical strain have also been used to mimic the stretching and strain of an *in-vivo* situation where cells elongate akin to grooves. For example, in the arterial basement membrane. However cell reaction in this simile, varies from parallel *in vivo* (for endothelial; probably due to shear stress) to orthogonal *in-vitro* (Buck 1980). Orthogonal orientation is also dependent on the amplitude of the stretch (Takemasa, Sugimoto et al. 1997; Takemasa, Sugimoto et al. 1997) and has been hypothesised to be a compensatory effect. Although stretch is not topographical, the induced morphology is similar and one can draw parallels with the causative effect. It must be made clear that, although the elongation was similar, it does not necessarily occur via the same mechanism and one can only speculate on any parallel mechanism at this moment in time.

More recently, divergent results have been observed in stretch experiments where the elongation was parallel rather than orthogonal to the cyclical strain. This was dependent on the magnitude and cycling parameters and on "when" the strain was applied. Ultimately, a hybrid of flexibility and topographical guidance would be ideal in some *in-vivo* situations for a biomaterial, e.g. vascular grafting. Primarily for "bluesky" research, a grooved substrate has a more homogeneous reaction and is better for investigating the contact inhibition hypotheses, since a flexible substrate may have localised differences in flexibility. Curtis and Varde (Curtis and Varde 1964) initially used the parallel features of diffraction grating replicas, and Rovensky (Rovensky, Slavnaka et al. 1971), using similar cells to Buck (Buck 1980), showed

parallel alignment rather than orthogonal to an aligned topographic cue. However, it was not until later, when microfabrication allowed surfaces with various accurately defined topographies, that contact inhibition on micro and nano features could be investigated fully (Clark, Connolly et al. 1991). Now it is possible to manufacture accurate nano features in many guises. These range from grooves to pillars to pits. With these well-defined fabricated substrates, followed by surface treatment, one can eliminate the differences in "wettability" and adhesion seen on topography with variable depth.

The reaction to patterned surfaces, in comparison to the more usual flat surface, has informed on many possibilities for studying basic cell biology (Curtis and Clark 1990) (Singhvi, Stephanopoulos et al. 1994). For example, gene expression (Chou, Brunette et al. 1995; Xynos, Edgar et al. 2000) and elctrophysiology (Ternaux, Wilson et al. 1992). Clarke and others discerned that groove-depth variance affects orientation and elongation (Clark, Connolly et al. 1991) and Britland showed the hierarchy of topography versus chemical guidance (Britland, Morgan et al. 1996). Following Britland's work, one might successfully argue that any future research should concentrate on micropatterned surfaces (and indeed this is a focus of some colleagues). However, there are many in-vivo situations where a tough, rigid, and non bioactive material is required that still allows tissue integration. The most obvious being hip prostheses, cardiac stents and urethral/colonic catheters. Here research (which has now become the field of "Tissue Engineering") has concentrated mainly on understanding cellular recognition of these potentially implanted biomaterials, their surfaces (Boyan, Hummert et al. 1996), and their integration to an *in vivo*

system (denBraber, deRuijter et al. 1997). There nevertheless are still parallels with the original work by Paul Weiss and Michael Abercrombie and the more fundamental reaction of cells to a topographical cue.

There is a great deal to be discovered in formation of tissue, both in development and in tissue augmentation via prosthetics or accelerated regeneration. Therefore, when investigating surfaces with potential for implantation or as a model system, consideration must be given to the natural counterparts and their biological mechanisms.

Substrates and Specific Cell Reactions

The types of substrate for tissue engineering and topographical analysis have varied, as methods of fabrication have become either technically or economically viable. Initially Curtis and Varde (Curtis and Varde 1964) used replicas of diffraction gratings as their grooved/ridged substrate. However, with the onset of the microelectronics industry and photolithography, defined topographies have become widely available. Even so, some researchers are still using hand cut grooves that will obviously have nanometric sub-features. This should not be necessary since there are readily available inexpensive substrates with micrometric grooves, which do not require the use of photolithography. The variety of topography used past and present, includes; pillars/spikes (Rovensky, Slavnaka et al. 1971) (Turner, Dowell et al. 2000), nano-scale pits (curved and shear sided) and pillars (Curtis, Casey et al. 2001). Others include, colloids (Wood, personal communication), flexible grooves (M Riehle, personal communication) and groove/pillar composite hexagonal patterning (Kam,

Shain et al. 1999). Tissue substitutes are now being constructed which embrace desirable tissue characteristics for example, Bioglass (Xynos, Edgar et al. 2000; Xynos, Hukkanen et al. 2000), which enhances the proliferation and deposition of mineralized collagenous matrix; and hydrogels (Lee and Mooney 2001), used to mimic the gelatinous environment of the cartilage. Both have topographical structures in the micro and nanometer range but mimic the general properties of the *in-vivo* environment, specifically rigidity, and strength combined with flexibility. In some circumstances, it is not just integration but also control of cell reaction which is desirable, for example, increasing proliferation or accentuating differentiation and apoptosis. This can be achieved by ECM patterning (Morla and Mogford 2000) or by altering the adhesive areas by contact printing or photolithography (Chen, Mrksich et al. 1997).

With respect to adhesion modulation, Gallagher (Curtis, Casey et al. 2001) (Wilkinson, Riehle et al. 2002) produced nano-pits by inverse patterning a biodegradable substrate (poly-e-caprolactone) from a pillared master. This selectively prevented cell adhesion, even though a confluent monolayer was able to form on the immediately surrounding flat surface. This seminal work illustrated how simply altering the topography of a substrate could have diametrically opposite effects on a cell population. Indeed, down-regulation of adhesion on these selective surfaces could be utilised in regulation of tumour invasion, since angiogenesis is required for tumour growth and branching capillary endothelial need adhesion for tubule formation. Perhaps coating a tumour in such a surface could modulate the

malignancy. If it turns out that the lack of adhesion was due to apoptosis, possibly a similar surface could be optimised to target tissue by simply inducing cell death in proliferating tumour by inducing apoptosis upon contact.

However, the focus of this thesis was on parallel grooved structures and their potential uses. Existing practical applications of grooved guidance included, the inhibition of orthogonal migration to prevent epithelial ingression in dental prosthesis (Chehroudi, Gould et al. 1992), and for tendon repair (Wojciak-Stodhart, Crossan et al. 1995) (Wilkinson, Curtis et al. 1998). There are many potential applications. For example in conjunction with growth factors (chapter 3), or by modulating the topography of an artificial basement membrane (Babu and Wells 2001), one could perhaps utilise directed movement in the treatment of ulcers; a significant problem in the care of bedridden patients and diabetics.

The structures used in this thesis were made on my behalf by Mrs Mary Robertson, Dept of Electrical and Electronic Engineering, Glasgow University, using photolithography and masking technique described in figure 2.1.

Grooved Topographical Guidance

In general, parallel topography induces an elongated morphology (figure 1.1) and directed movement in many cell types including fibroblasts (Clark, Connolly et al. 1991; Oakley and Brunette 1993), epithelial (Clark, Connolly et al. 1991)(Oakley and Brunette 1995; Brunette and Chehroudi 1999), neuronal (Clark, Connolly et al. 1991) (Nagata, Kawana et al. 1993) (Rajnicek and McCaig 1997) and macrophage cells

(Wojciak-Stothard, Madeja et al. 1995). The elongation reaction to the grooves is depth dependent (Clark, Connolly et al. 1991) and cell type dependent (Clark, Connolly et al. 1991). Cellular morphology is also affected by cell-cell contact (Clark, Connolly et al. 1991). Clark and Connolly found that there was extension and orientation in single epithelial cells but those cells that were part of an epithelial islet were only extended on the outer rim of the cell clump. Internal cells were unaligned.

The groove type can be straight edged (Curtis and Wilkinson 1997; Curtis and Wilkinson 1998) or V shaped (Brunette 1986; Brunette 1986). The anchorage dependent morphology of cells is synonymous with activation (Howe and Juliano 2000), proliferation (Rescan, Coutant et al. 2001) (Kononen, Hormia et al. 1992), functional integrity (Sechler, Corbett et al. 1998) and survival itself (Chen, Mrksich et al. 1997). Understanding these reactions has great significance, not only in research-biology but also medicine; specifically prosthetics, where an implant might be expected to remain in-situ for many years and sustain the integration of functional tissue. Indeed "highly polished" hip-implant ball and socket prostheses have nanotopography of approximately 20 to 50nm. In laboratory research, topography may have a bearing in standard tissue culture, where the roughness of the culture plate surface will affect cell adhesion and perhaps proliferation and outside-in signalling pathways. Fortunately for research, glass coverslips, used ubiquitously in biochemical analysis as a substrate, are extremely flat and homogeneous when measured by atomic force microscopy.

Migration

The migration of various cell types is affected by parallel grooves. Wojciak-Stodhard determined that macrophage cells increased in speed on 10μm wide x 0.5μm and 5μm deep grooves and their persistence of movement was greater. Interestingly, the speed was greater on the shallower grooves (Wojciak-Stothard, Madeja et al. 1995) (Hollander, Schmandra et al. 2000). B10D2 and HGTFN endothelial plus tendon-epitenon also have increased speed along grooves (Curtis, Wilkinson et al. 1995).

Elongation and Orientation

On square-edged grooved topography, the elongation and orientation of many cell types is depth dependent (Clark, Connolly et al. 1991). One might argue (and some researchers have speculated) that this orientation was due to the increased surface area that vertical edges present to the cell and the additional right angle at the bottom of a groove. However as shown in the next chapter and in the signal transduction experiments in chapter 5; this increase in elongation was not linear. Nor was it a gradual geometric extension that one would expect if there was a cumulative response to increased surface area allowing for greater adhesion.

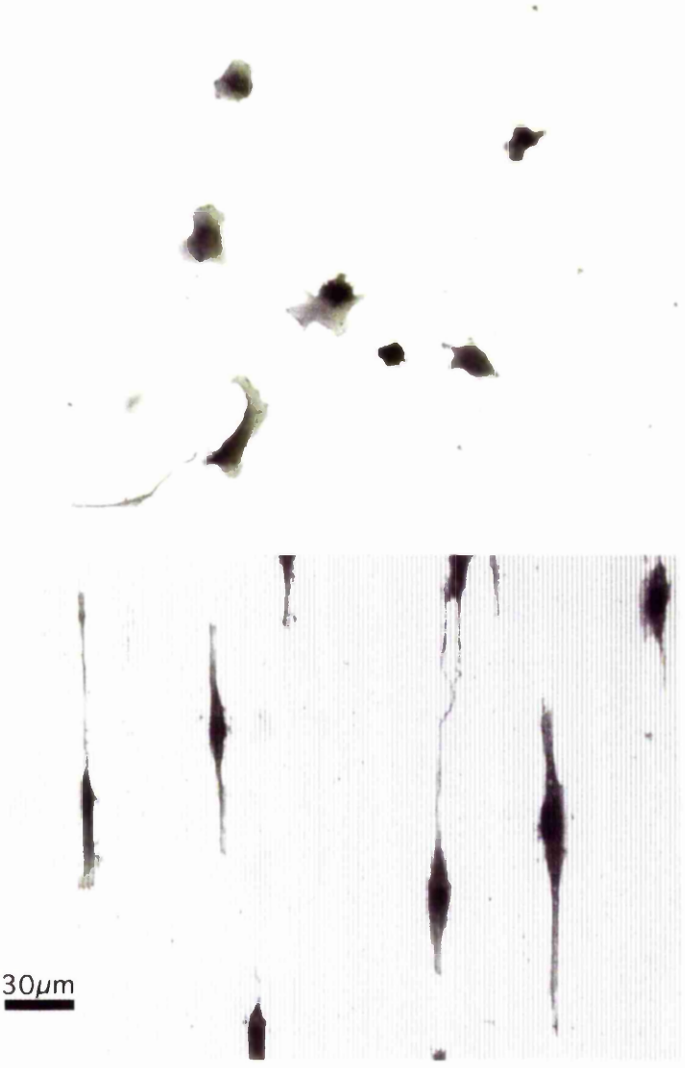

Figure 1 HGTFN endothelial cells grown on 970nm- deep vertical grooves and on a flat surface.

The grooves (bottom) orient the cells in the groove direction (vertical) compared to the flat surface(top). The cells also change their persistence of movement along the grooves. In addition the speed of cells in general was increased from the random walk observed on a flat surface.

Adhesion

Differing topography evokes alteration in adhesion compared to a flat surface. Even on identical substrates, the modulus of reaction was cell type dependent. Osteoblasts will have greater adhesion on nanometric surfaces (at 100nm) in stark contrast to fibroblasts that have reduced adhesion on identical features (Webster, Ergun et al. 2000). Macrophage cells have a significant reaction to nanotopography that was ineffectual for epithelial (Wojciak-Stothard, Curtis et al. 1996). Therefore, one can speculate that the mechanisms for adhesion were different. Clarke et al (whose work was the inspiration for the directed movement in this thesis) showed that MDCK epithelia had different reactions to grooved topography, whether they were individual cells or multicellular islets (Clark, Connolly et al 1991). Considering the major signalling events that occur in cadherin-adherens junctions, that regulate the basal apical ion channel polarisation, it was no surprise that side-side junctions could alter the topographical reaction. Mainly, the adhesion complex used as the "model system" is the focal adhesion. Focal adhesions are multicomponent protein complexes that transduce extracellular adhesion into anchorage strength via actin stress fibres. Focal adhesion complexes also interlink adhesion to functional second messenger cascades via accessory proteins e.g. FAK. The reader is referred to three comprehensive reviews by Burridge and Chrzanowska-Wodnicka (focal adhesions)(Burridge and ChrzanowskaWodnicka 1996) Erriki Ruoslahti (adhesion sequences) (Ruoslahti 1996) and Aplin *et al* (signal transduction) (Aplin, Howe et al. 1998, 1999).

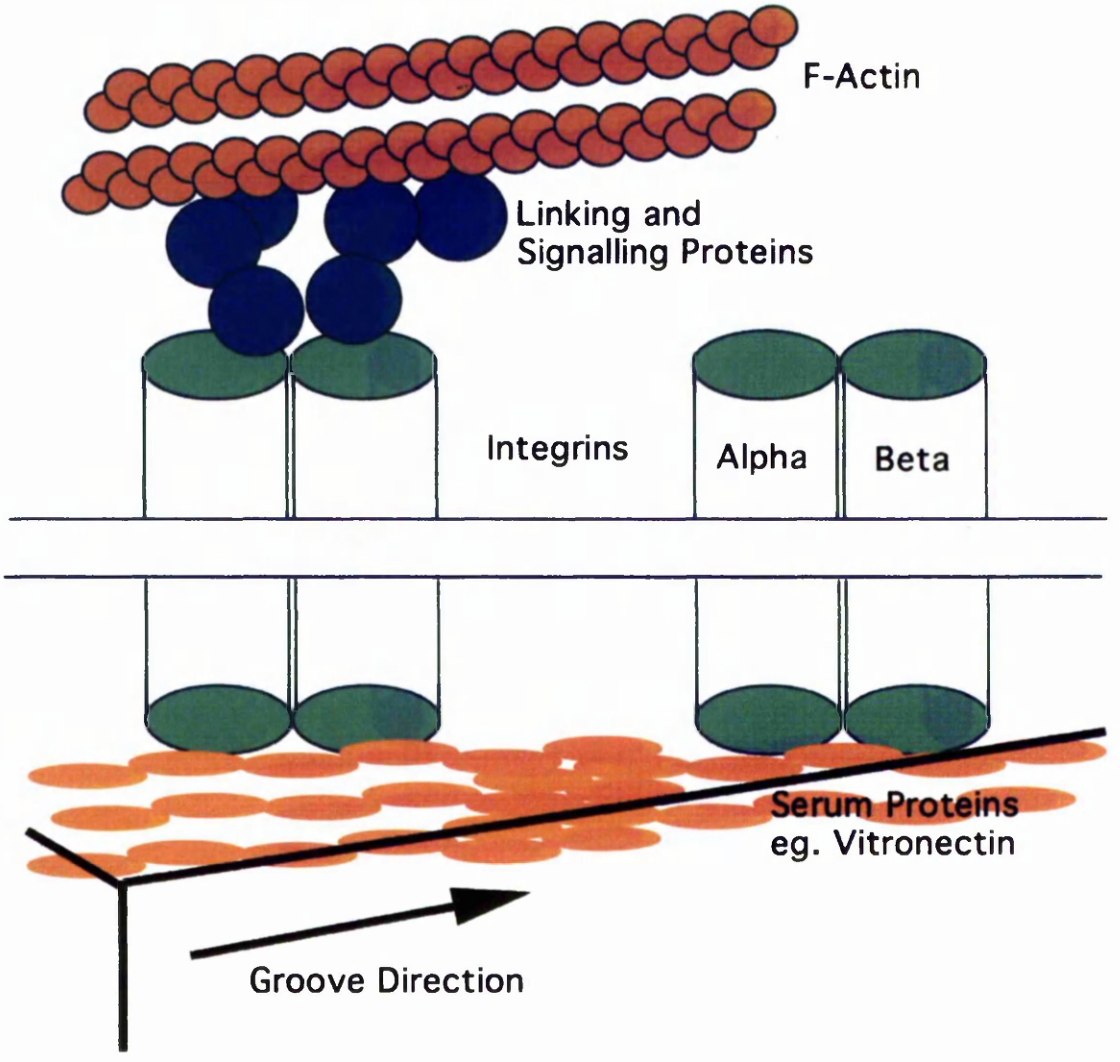

Figure 1.2 Cell Adhesion mechanism on grooves

One way in which cell elongation may occur along a groove, is preferential alignment of serum proteins and/or focal contact molecules at the groove edge. The mechanism is not clear yet, however, there is a clear correlation with the extracellular groove edge and alignment of actin within the cell. The actin binding proteins and integrins are likely progenitors of the effect.

Mechanisms

Surface energy plays no role in elongation (Denbraber, Deruijter et al. 1995) but affects other cellular functions like proliferation (Denbraber, Deruijter et al. 1995) and reactive ion oxidative bursts in macrophage (Baier, Axelson et al. 2000). To date, there is no definitive mechanism to account for topographically induced elongation. Naturally potential targets for elongation on grooves have included focal adhesions. Although these do have a directionality, aligning their major axis in the line of spreading, this has not been shown to be significant or to act as the fundamental driving force. Also, there is no evidence for initial integrin condensations being able to sense any direction of grooves. Curtis has suggested that asymmetric chloride channels could offer the link by acting as directional stretch receptors. Blockage of these receptor's expression via antisence mRNA has shown promising results. (Curtis ASG personal communication). Recently Kaverina (Kaverina, Krylyshkina et al. 2002) showed that microtubules were targeted to areas of applied tension and postulated that there was a stress dependent feedback to the microtubule system.

Aims

The principle aim of this research was to study the intracellular reactions that govern the morphological reactions of cells on parallel grooves with micro- and nano-metric dimensions. Although literature exists investigating changes of the gross morphology of cells on grooves, the signalling mechanisms involved in this reaction have yet to be determined. This thesis expands upon previous work using MDCK epithelia on groove type topography, which showed that changes in cell morphology were dependent on the degree of cell-cell contact (Clark, Connolly et al 1991).

This thesis aims to:

- Investigate the effects that grooves of varying depth (micro- and nanometric) have on the morphologies (cell-width, length, area and orientation) of single and small groups of MDCK epithelia and how this affects their migration. Also how the morphology of MDCK epithelia on grooves is reflected in the cytoskeleton (F-actin, microtubules and intermediate filaments).
- Examine if the various parameters defining endothelial cell morphology such as cell-width, length, area and orientation were affected over time and by groove depth.
- Explore how endothelial cell morphology was regulated, by combining the use of specific inhibitors to identified signalling pathways, with the use of grooves to influence cell morphology in a predefined way.
- Develop an explanatory model for the reaction of endothelial cells to grooved topography.

Chapter 2

Cell adhesion and elongation on nano and micro grooved topographical surfaces.

Introduction

Cells encountering a substrate with parallel grooved topography orient their major axis in the direction of the groove. This was described briefly in chapter 1. The cell orientation is usually accompanied with migration in the same direction, although the mechanism of this reaction has yet to be determined. Indeed, as will be shown in chapters 3 and 4, elongation on topography was not necessary for the underlying substrate to facilitate cytoskeletal alignment or directional migration. The reaction of various cell types to micro-topography is well documented, (Rovensky, Slavnaka et al. 1971) (Clark, Connolly et al. 1990) (Wojciak-Stothard, Madeja et al. 1995). However, with the exception of Clark (Clark, Connolly et al. 1991) and Wojciak-Stothard (Wojciak-Stothard, Curtis et al. 1996) there has been little research on the effect of nanometric topography. Clark investigated the alignment and elongation of BHK_{21} fibroblasts and MDCK epithelial cell lines and found that single MDCK cells aligned to the same extent on 100nm 210nm and 400nm deep grooves. However, the BHK alignment increased with a near linear trend, from flat through 100nm 210nm to 400nm. He also found that MDCK cell length was dependent on grating depth. There are a multitude of nanometric features a cell comes into contact with, e.g. collagen fibrils (67nm banded fibrils), laminin (~70nm long) fibronectins, proteoglycans and even the nanometric features of bio-implants.

In this chapter, the hypotheses that HGTFN endothelial would elongate in a depth dependent manner, like other cell types, was assessed. I used depths ranging from 50nm to 5μm. Whether the elongation and orientation would increase with groove depth or whether there would be a depth threshold at which cells would align was yet to be determined. In addition the reaction to Protein translation inhibition was also determined prior to subsequent gene expression and signal transduction studies. The time-course for HGTFN cell adhesion was 3 hours to determine the reaction as cells spread and 18 hours when fully spread.

I also confirmed the MDCK cell reaction described previously by Clarke (Clark, Connolly et al. 1991), characterising the morphology for further analysis on directed movement of the cells as single cells or cell islets.

Materials and Methods

In this chapter detailed cell culture, staining procedures and methods of analysis are described. Specific techniques relating to a particular chapter will be described in those chapters.

Photolithography

Structures were prepared by Mary Robertson (Electronic and Electrical Engineering, University of Glasgow) using photolithography methods described by Wojciak-Stothard (Wojciak-Stothard, Curtis et al. 1995; Wojciak-Stothard, Curtis et al. 1996). See figure2.1 for an overview.

Cell lines

p388D1 Macrophage Like Cells

p388D1 mouse macrophage were routinely cultured in the Centre for Cell Engineering laboratory, University of Glasgow, but were originally a gift from Prof. P Bongrand, Marseilles

HGTFN Cells

HGTFN endothelial were from departmental stock and routinely cultured in the Centre for Cell Engineering.

MDCK Cells

Maden Darbey Canine Kidney (MDCK) for initial experiments were from departmental stock. However, fresh cells were later bought from the European

Collection of Cell Cultures catalogue number 84121903 (passage 12) as a growing culture for experimental work. These were expanded at passage 13, trypsinised and resuspended in 90% foetal calf serum + 10% dimethyl sulfoxide. These suspensions were split into 3 X 1ml vials/25cm^2 tissue culture flask, then cooled to –70C in a polystyrene box. Following the overnight cooling they were then transferred to liquid nitrogen for long-term storage. For experiments, cells were used at passage 16-30.

Cell Culture Solutions and Final Media

All solutions, except MDCK cell antibiotic mix, cryopreservant solution and final media, were prepared by Graham Tobasnick and Gordon Campbell, Division of Infection and Immunity, University of Glasgow.

Eagles Water

Milipore^{TM} reverse osmosis (MiliQ RO) purified water that was subsequently autoclaved and stored at 4^{O}C.

Hepes Water

1 litre MiliQ RO water plus 5.25g HEPES (N-2 hydroxyethyl piperazine-N' 2 ethane sulfonic acid) (Sigma) pH adjusted to pH7.5 and stored at 4^{O}C.

7.5% Bicarbonate

7.5g Sodium bicarbonate/100 ml water then filter sterilised.

HEPES saline Buffer

Sodium Chloride	8g

Potassium Chloride	0.4g
D-Glucose	1g
HEPES	2.38g
Phenol-Red Sodium Salt	0.1g

Made to 1 litre with RO water and pH to 7.5

Versene Buffer

Sodium Chloride		8.g
Potassium Chloride		0.4g
D-Glucose	Sigma	1.g
HEPES	Sigma	2.38g
Phenol-Red		0.1g
EDTA	Sigma	0.2g

Made to 1 litre with RO water and pH to pH7.5

General Antibiotics mixture

Glutamine	Gibco	144mM
AmphotericinB		11.9μm
Penicillin	Gibco	100μg/ml
Streptomycin	Gibco	100U/ml
Bicarbonate	Gibco	7.5%

PBS

5 Sigma PBS tablets added to 1litre RO water and pH adjusted to pH7.3

ITS (Insulin, Transferrin, Selenite solution)

5 μg/ml for transferrin, Insulin and 5 ng/ml selenite. lyophilised transferrin was dissolved in water (pH adjusted to pH3 with acetic acid). The solution was filter sterilised and stored at -20°C.

Trypsin

Sterile trypsin Gibco 0.25% W/V was dissolved in Hepes Saline (stored at $-20^{O}C$). For cell dissociation; 0.5ml trypsin solution was added to 20ml versene.

Media Recipes

MDCK Cell Media (MEM)

MEM (Sigma)

Glutamine	Gibco	200mM final concentration
Streptomycin	Gibco	100μg/ml final concentration
Penicillin	Gibco	100U/ml final concentration

HGTFN Endothelial Cell Media (Ham's F10)

Hepes Water		180ml
HamsF10 10x	Gibco	16ml
Antibiotics mix		5ml
Foetal Calf Serum	Gibco	6ml

ITS		2ml
Bicarbonate mix		1ml

p388D1 Mouse Macrophage Cell Media (RPMI)

HEPES Water		180ml
RPMI 10x	Gibco	16ml
Antibiotics mix		5ml
Calf Serum		20ml
Bicarbonate mix		5ml

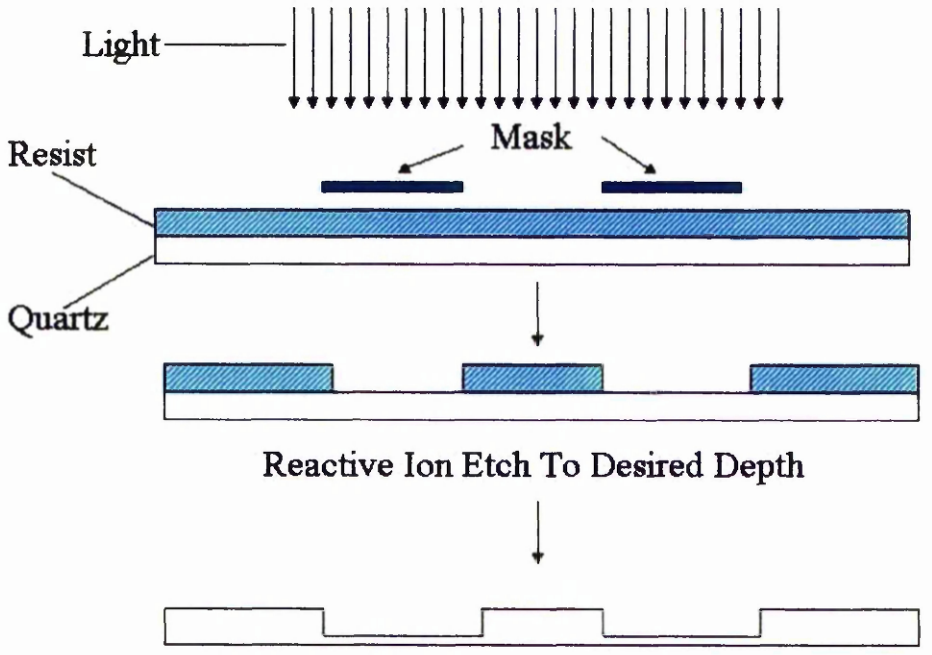

Figure 2.1 Method of groove manufacture.

Schematic showing how a grooved surface was made using negative etching photolithography. A quartz sample was coated with a "resist" (which is modified by light). To create a pattern, a patterned "mask" was placed above the resist and the resist "hardened" with light excitation. Then the resist was removed with solvent. Once a pattern was created, the mask was removed and grooves etched where the resist had been removed. Different depths were created by altering the etch time. After the removal of the remaining resist, the samples were blanket etched to ensure uniform surface chemistry.

Methods of Routine Culture

HGTFN Cell Culture

HGTFN endothelial cells were cultured at 37^{O}C in 25cm^{2} Falcon tissue culture flasks with Ham's F10 media and, unless passaged within 3 days, were opened for 10-15 minutes to allow re-oxygenation of the media. For subculture, the cells were washed twice with hepes saline (37^{O}C) to remove serum (a trypsin inhibitor) then 5ml trypsin-versene (37^{O}C) was added for 30 seconds to 1 minute (or until cells began to round up) and excess trypsin-versene poured off. The cells were returned to a 37^{O}C hot-room and observed using phase contrast microscopy until detached. Immediately upon detachment, 15ml of HAM's F10 + serum (pre-warmed to 37^{O}C) was added to neutralise the trypsin. The cells were then pelleted by centrifugation for 4 minutes at 1000RPM and 4^{O}C. Once pelleted, the supernatant was removed and the cells resuspended in 10ml of HAM's F10 then plated in 25cm^{2} tissue culture flasks.

MDCK Cell Culture

MDCK cells were cultured at 37^{O}C, passaged every three to four days and re-seeded at medium density (approximately 20% flask coverage). Initially, the cells were washed with hepes saline at 37^{O}C. If the cells were nearly confluent, they were incubated in Versene (37^{O}C) for 5 minutes to "loosen" the Ca^{2+} dependent adherens junctions. Although this depletes calcium, it reduced the time of exposure to trypsin. They were then subcultured by adding 5ml trypsin versene (37^{O}C) (most of which was removed after 10 seconds leaving a thin film) until detached from each other's

sides. They were further incubated for up to 5 minutes or until released from basal adhesion by gently tapping the flask. Following detachment, they were centrifuged, re-suspended in MEM + 10% FCS ($37^{O}C$) and plated at approximately 10-15% confluence. An additional 5ml of 100% CO_2 was sterile filtered into the flask for buffering.

p388D1

p388D1 macrophage were cultured at ($37^{O}C$), passaged every 3 days and seeded at approximately 10% confluence. Due to the low adherence of these cells, they were detached from the flask by tapping by hand. The cell suspension was centrifuged at 1000rpm for 4 minutes to pellet the cells, which were resuspended in RPMI media ($37^{O}C$) and platted into $25cm^2$ tissue culture flasks.

Cryopreservation of stock cells.

Cells were detached, centrifuged and resuspended as previously described. Where trypsin was used, the cells were given an additional medium resuspension. They were then centrifuged and re-suspended in 90% FCS + 10% dimethyl sulfoxide. To reduce the cooling rate, cell suspensions were incubated for four hours at $-20^{O}C$ in a foam surround within a sealed polystyrene box then overnight at $-70^{O}C$. This method was used as a temporary storage situation for three-month working stock. Additional vials were transferred to liquid nitrogen for long term storage.

Cell Counting

Cell counts were performed using a haemocytometer (Fuchs-Rosenthal ruling). The eight cells volume was $1x10^{-4}$ml. Therefore 32 squares were counted, for better averaging.

Cell Seeding On Structures

HGTFN cells and MDCK cells were seeded directly onto flat, 50nm, 100nm, 300nm and 970nm deep parallel square angle grooves in a media droplet (approximately 300μl of media with the required cell density) and allowed to attach for 30 minutes (to prevent selective adhesion of a subset of cells). Once the cells had adhered to the surface, the remaining media was added and the cells incubated for a total of 3 hours and 18 hours (HGTFN cells) or until the diversity of cell morphologies could be assessed (MDCK cells). HGTFN cells were then formalin fixed and stained with Coomassie Blue. MDCK cells were video taped for movement analysis. The cell parameters measured are described later. The structure dimensions were either 12μm wide x 5μm deep or small structures with 1μm, 2μm and 4μm wide grooves which had different depths of 50nm, 100nm 300nm or 970nm etched.

Surface Cleaning and Drying

Each structure or glass cover slip was cleaned with Caro's Acid (permonosulphuric acid), a mix of 1 part 30% (100 volume) hydrogen peroxide and three parts 98%

concentrated sulphuric acid. The mixture was allowed to combine before the slides were added gradually into the hot mixture (temperature was approximately 80^{O}C) and cleaned for 20 minutes. Subsequently, each structure/slide was washed in MilliQ water 3 times for 1 minute then finally allowed to sit for twenty minutes. This ensured removal of any residual Caro's acid from the surface.

The cleaned structures were immersed in 70% ethanol for sterilisation, then dehydrated in 100% ethanol to aid a residue free surface following air dying. Following this the structures were placed in 60mm tissue-culture petri-dishes and air dried for 20-30 minutes in a laminar flow sterile tissue culture hood.

Cell staining

Coomassie Brilliant Blue

Methanol	225ml
Glacial Acetic Acid	50ml
Water	Added to 500ml
Coomassie Brilliant Blue R-250	1.25g

Stirred for 30 minutes and filtered through Wattman number 1 filter paper.

Cells were washed in 1xPBS (pre-warmed to 37^{O}C) and fixed in 4% buffered formalin (37^{O}C) for 5 minutes. They were then washed with 1xPBS and stained with Coomassie Brilliant Blue for 1-2 minutes or until the required stain density was achieved. The excess stain was rinsed off with water and destained with either water or acetic acid/methanol.

Protein and Nuclear Stain

This method (developed by Volberg et al. 1994) was used when nuclear and cell morphology was assessed or where the grooves interrupt the detection of the cell morphology. Cells were fixed with pre-warmed 4% buffered formalin for 5 minutes allowing membrane protein cross -linking. For Texas-red, 150µl (1mg/ml in dimethyl-formamide) per 6ml media was added directly to the fixative for 10 minutes (following the initial 5 minutes). This bound the Texas-red onto the proteins. Excess stain was removed by washing with 1xPBS. When Hoescht 33258 was used, it was combined with the Texas-red fixative solution at 1/200 dilution (5mg Hoechst 33258/5ml Ethanol stock).

Image capture

Images of HGTFN cells were captured using a Hamamatsu CCD camera and an Argus20 digitiser in windows bitmap format 928x680x8bit resolution. This was attached to Leitz Diavert, Zeiss Axiovert and Vickers M15 microscopes.

Images of MDCK cells were captured at 4x and 10x magnification (Zeiss Axiovert 20 microscope) by CCD camera in SVHS format on a Panasonic time-lapse video recorder. The individual frames were captured on a Macintosh PowerPC Computer (fitted with a digitising card) using NIH image and Object Image analysis packages and converted to tiff format stacks and QuickTime movies.

NIH can be freely downloaded from http://rsb.info.nih.gov/nih-image

Object Image (an NIH modification) http://simon.bio.uva.nl/object-image.html

Cell parameter measurement

Cell parameters were measured using NIH Image for Macintosh and an analysis macro written by Dr. Mathis Riehle (Centre for Cell Engineering). The macro measures the maximum axis, minimum axis, cell area, angle of orientation. Data was correlated using an Excel (Microsoft) spreadsheet template (written by Dr. Mathis Riehle) and statistical analysis calculated using Statview on a Macintosh Powerbook G3. The statistical tests used on each sample were ANOVA post-hoc tests (Fisher's PLSD, Scheffe and Bonferroni/Dunn) and the nonparametric Mann-Whitney test.

Results

HGTFN Cell Morphology after 3 hours Adhesion.

HGTFN cells were cultured on 2μm wide grooves of varying depths from 50nm to 970nm, and for two time points. A combination of the major axis length, minor axis length and alignment to the grooves were assayed. The following results show that, as the depth of the groove increases, the major axis increases, the minor axis decreases and the orientation becomes more aligned along the groove. There was a significant distinct, switching of alignment and elongation on the grooves as the depth reaches 300nm. This correlates with previous results on different cell lines. However, HGTFN cells do not respond to groove depth increases in a linear manner. The two time-points chosen for analysis were three hours, to detect early spreading reactions to the different depths, and eighteen hours for assessing whether there was any difference in the reaction once the cells had fully spread.

Figure 2.1 demonstrates that HGTFN cells on a flat surface and on 50nm and 100nm deep grooves had no orientation to the grooves. On 300nm deep grooves the reaction over 3 hours was enough to produce significant alignment of the cells along the groove (figure 2.4 and figure 2.5). The area measurements in figure 2.3 were interesting. These showed that there was a significant difference (compared to a flat surface) in the 100nm sample and 300nm sample but not in the 970nm sample. The 970nm non-significance was easy to explain by considering the major and minor axes (figure 2.5) where the increase in extension along the groove was compensated by the reduction in the width. This was perhaps due to a tension effect. An analogy would be

a fabric weave, where a strong force stretching in one direction would counteract the weaker force in the lateral direction. This hypothesis is speculative regarding the force differences exerted by a cell on different groove depths. It would require further analysis on a suitable substrate to prove it, such as flexible grooves with beads to measure the force by bead deflection. This effect was not the focus of this thesis but is none the less an interesting consideration. The significance in the 300nm sample could be attributed to an increased spreading of the cell in one direction being enough for mild extension without pressing constraints on lateral adhesion. Following on from the previous speculation, it may be suggested that there are different levels of force generated by cells on different groove depths. The significance of the increased spreading on 100nm deep grooves without orientation implied that HGTFN cells were able to spread better at short time-points (3 hours) on nanometric grooves. On the 100nm deep grooves only the major axis length was significantly different. This may not seem striking but becomes more relevant when the chapter 5 results are taken into consideration. This spreading increase occurred even when other reactions seen on deeper grooves (orientation and extension along grooves) were not evident. When the ratio of major axis length to minor axis length was compared, figure 2.6, it was clear that the 50nm and 100nm deep grooves did not alter the "roundness" of the cells compared to the flat sample. On the 300nm deep and 970nm deep grooves there was a difference. When assessing this result, the orientation must be considered to determine whether the bipolarity was extending along the groves and figure 2.4 demonstrates this clearly for the 300nm and 970nm deep grooves.

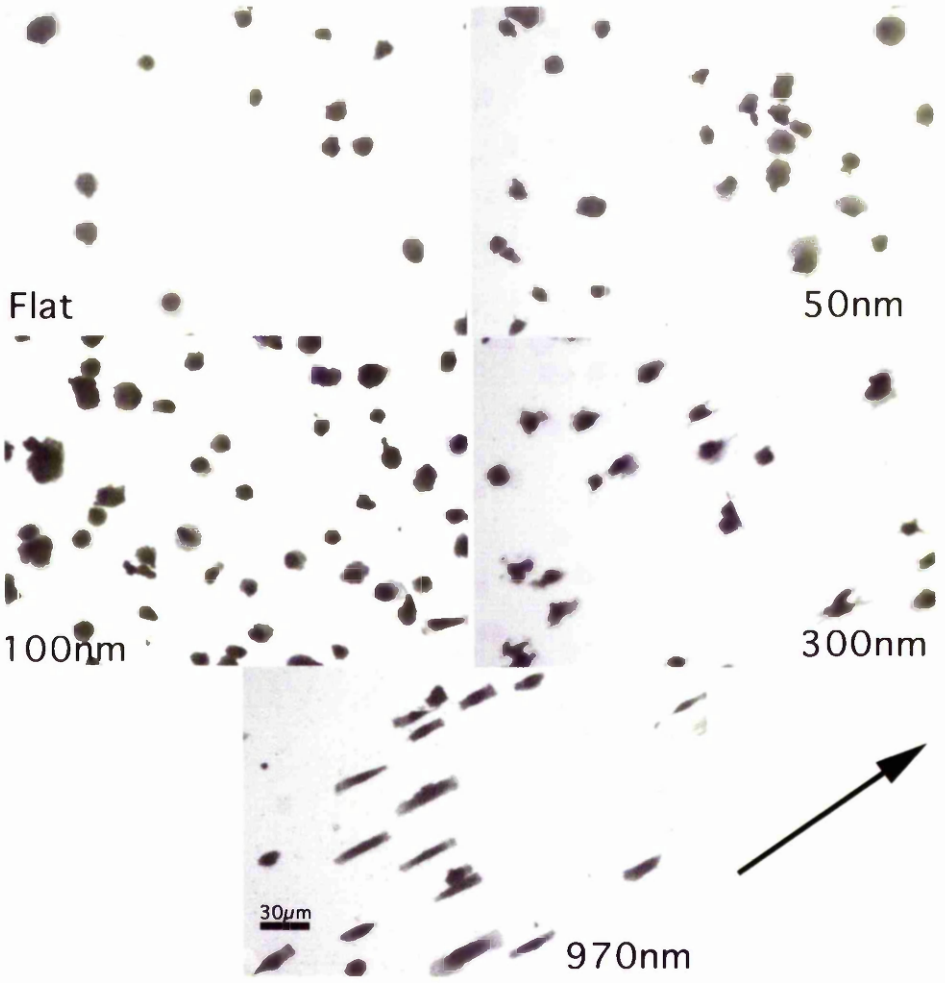

Figure 2.2 Morphology of HGTFN cells on 2μm wide grooves with different groove depths.

The cells were cultured for 3 hours on; flat, 50nm, 100nm 300nm and 970nm deep grooves. The groove direction was 45^{O} (bottom left to top right). There was no alignment of the major axis on the flat, 50nm nor 100nm sample. On the 300nm deep sample and significantly on the 970nm sample there was elongation along the grooves. Arrow indicates the groove direction.

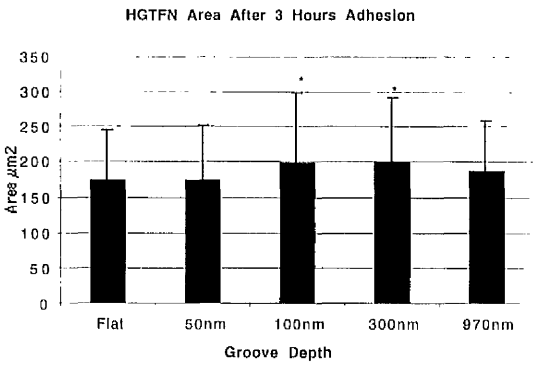

Area	Avg	SD	Median	n
Flat	175.3	71.9	157.9	319
50nm	175.3	76.7	158.0	143
100nm	199.6	100.8	170.8	346
300nm	201.8	91.4	184.9	241
970nm	187.3	74.0	168.9	317

Figure 2.3 Area of HGTFN cells after 3 hours spreading on 2µm wide grooves.

The significant differences (=P-value<0.01) in the four grooved samples when compared to a flat surface are for 100nm and 300nm deep grooves. These were significant using ANOVA tests, however, only the 300nm sample was significant using a non-parametric test. These statistics do not give a true reflection of elongation on grooves since area may change but there are significant differences in the major and/or minor axes.. The reduction in area on the 970nm sample compared to the 300nm was due to width reduction.*

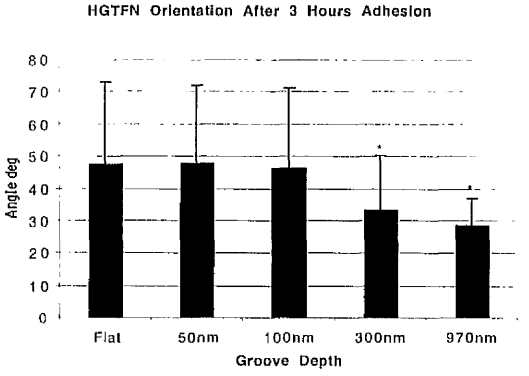

Angle	Avg	SD	Median	n
Flat	47.4	25.6	48.8	319
50nm	47.8	24.6	46.7	143
100nm	46.2	25.3	47.4	346
300nm	33.4	17.1	32.3	241
970nm	28.9	8.4	28.4	317

Figure 2.4 The orientation of HGTFN cell's major axis on 2μm wide grooves where the long axis of the grooves is 0^0

This graph shows that there was no significant alignment to the groove direction in the 50nm and 100nm deep grooves when compared to the flat sample. The orientation of HGTFN cells on 300nm and 970nm deep grooves was significantly aligned along the grooves. Non alignment was indicated by the spread of data from 0-90 degrees and the mean of 45 degrees from the groove. Alignment was indicated by the bar being closer to zero degrees from the groove direction and having a smaller angular data range.

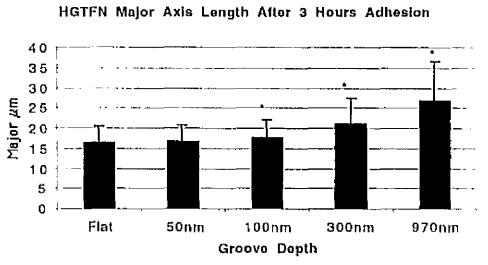

Max Axis	Avg	SD	Median	n
Flat	16.6	3.9	15.6	319
50nm	16.8	4.2	15.6	143
100nm	17.8	4.5	16.8	346
300nm	21.2	6.4	20.1	241
970nm	27.0	10.0	25.0	317

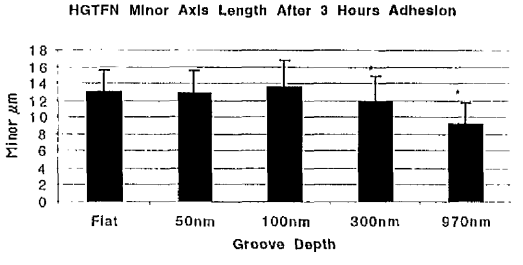

Min Axis	Avg	SD	Median	n
Flat	13.0	2.6	12.8	319
50nm	12.9	2.7	12.7	143
100nm	13.7	3.2	13.3	346
300nm	12.0	3.0	11.6	241
970nm	9.2	2.6	8.9	317

Figure 2.5 Comparison of major and minor axis length of HGTFN cells on different groove depths following 3 hours adhesion on 2µm wide grooves.

*The major axis did not to differ from the flat sample until the grooves reached a depth of 100nm deep. The minor axis changes were significant in only the 300nm and 970nm samples. The 100nm deep grooves did allow the minor axis to increase but this was not statistically significant. There was no change of orientation in the 100nm sample (figure2.4), therefore the axes changes were attributed to adhesion and spreading differences. *=$p<0.01$*

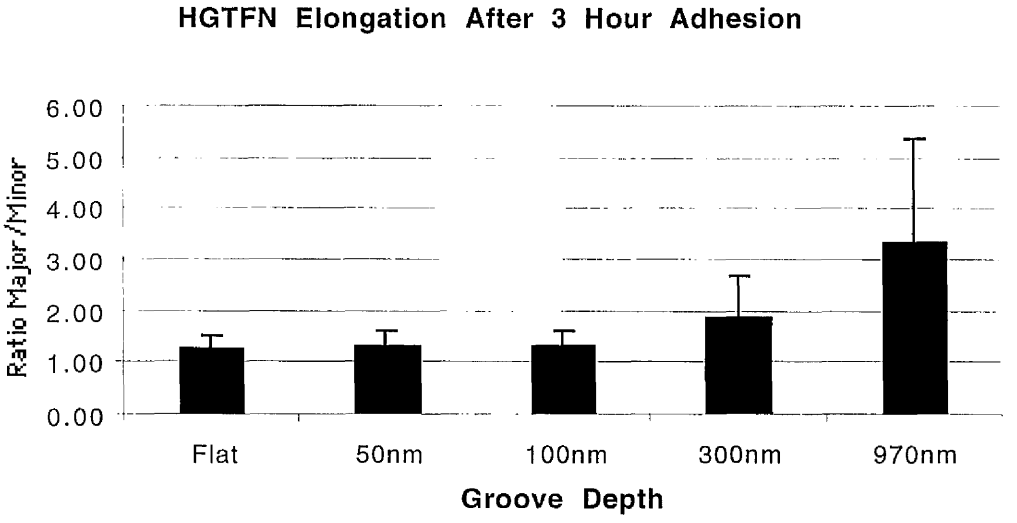

Figure 2.6 HGTFN cell elongation after three hours adhesion.

To determine the elongation of the cells the ratio of major axis to minor axis was compared. A threshold at between 100nm deep and 300nm deep, where the ratio deviated from the flat surface ratio was evident. In the flat, 50nm and 100nm sample the ratio was just over 1.0 and therefore the cells were almost round. In the 970nm sample the ratio was greater than 3.0 indicating an already elongated cell after three hours.

HGTFN Cell Morphology After 18 Hours Adhesion.

HGTFN cells were allowed to adhere for 18 hours in order for the cells to fully elongate. The morphology was shown in figure 2.7. The cell parameters were analysed in an identical manner to the 3 hour analysis. The reaction at later time-points was somewhat different to the three hour adhesion time-point. There were no significant spreading differences on the 50nm and 100nm deep grooves in any of the assessed parameters compared to the flat surface. Figure 2.7 and figure 2.8. Only the 970nm deep grooves showed a significantly different area compared to the flat surface but it must be noted that this was a reduction. The 300nm sample was not significantly different in area from a flat surface but closer inspection of the other parameters showed that there was a significantly different reaction compared to the flat, 50nm and 100nm samples, figure 2.9, 2.10 and figure 2.11. The conclusion that can be drawn was that the increase in major axis length was cancelled out by the reduction in minor axis width. One conclusion for the 970nm deep sample was the elongation along the groove of the major axis was not enough to counteract the reduction in width. Therefore, this resulted in a significant reduction in area. It would seem that there was a balance to be met in the axes extension and one possible scenario was that HGTFN cells are able to extend on the 300nm grooves a small amount. However, the extension was not strong enough to generate longitudinal tension that invokes a loss of orthogonal adhesion and subsequent lateral lamellipodia detachment. Therefore, the cells were still able to counteract the tension-induced narrowing at the lateral sides of the cell. The 970-nm samples on the other hand were

able to elongate to such an extent that they generate tension inwards and lateral to the nucleus of a magnitude such that the cell was unable to respond by spreading orthogonaly.

The major axis of the cells on the different grooves after 18 hours were different from the three hour sample. In the three-hour samples, cells were able to extend their major axis significantly from the flat surface on 100nm deep grooves, but as adhesion time increased, the flat and 50nm cells spread until there was no difference in the major axis. However, comparisons of figure 2.5 and figure 2.9 one can see that the major axis was larger after 18 hours and when comparing the ratio of the major to the minor, the ratio was doubled. This indicated that the 100nm deep grooves were able to extend the cells' major axis faster but after 18 hours adhesion the flat surface caught up. In summary, the only difference in the reaction of HGTFN cells to flat and 100nm deep grooves was a temporal shift and not a long-term difference. However, the reaction to 300nm and 970nm deep grooves was a permanent change of the individual parameters on the surface (longer time point experiments that I have done indicated the same results as the 18 hour samples).

The magnitudes of the major axis for the 18 hour samples was greater when compared to the three hour sample in all the samples. However, the minor axis change was not as large as the major axis increase. This indicated the cell width reaction to grooves was determined rather quickly on grooves but the elongation reaction took more time to reach its maximum.

Once the cells had become fully spread there was a significant difference in the ratios of the major to minor axes lengths. There was no difference in the reaction of the 50nm and 100nm samples compared to the flat surface; both had a "roundness" ratio of around two. This ratio was still double what was observed in the 3 hour a sample and supports the "catch-up" scenario.

Considering orientation, figure 2.11, there was no significant difference in the orientation of flat, 50nm and 100nm in and between both time points but orientation to the groove direction was evident in the 300nm and 970nm samples.

Results for the 300nm and 970nm samples show that the cell orientation was greater in the 970nm deep grooves and was significantly different from the flat sample. An additional finding was that the 18 hour adhesion generated more alignment in the 300nm and 970nm deep sample at 18 hour adhesion compared to three hours adhesion, figure 2.10 and figure 2.11.

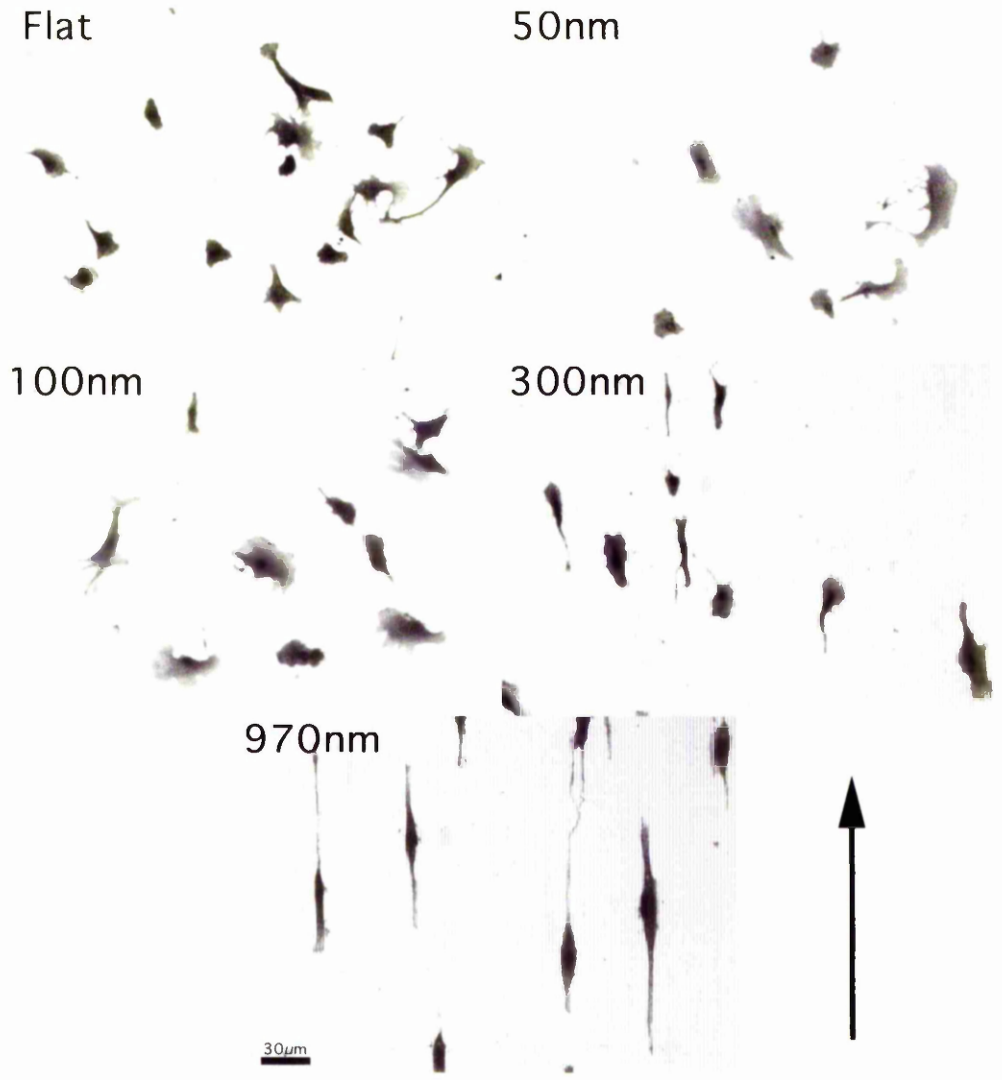

Figure 2.7 *HGTFN cells on 2μm wide grooves with different groove depths.*

The cells were cultured for 18 hours on flat, 50nm, 100nm, 300nm and 970nm deep grooves (groove direction was vertical). On the flat, 50nm and 100nm deep structures, the endothelial cells had a flattened morphology with well developed lamellipodia and no orientation to the vertical grooves. On the 300nm structure the cells were able to orient themselves to the vertical grooves. They possessed wide

lamellipodia at the leading edge and a certain degree of lateral spreading. However, on the 970nm deep grooves the cells were extensively elongated along the grooves. Any lateral spreading of cells on the 970nm deep sample was curtailed to the extremity of the leading edge and around the nucleus (probably due to the size of the cell body at this area and not actual lateral spreading). The orientation of the cells was also curtailed to the direction of the groove when the depth increases to 300nm. This was further accentuated as the depth increases to 970nm. Arrow indicates groove direction

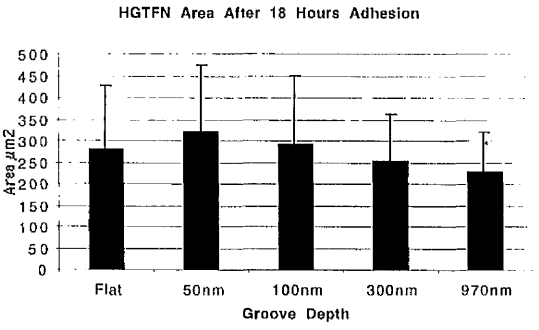

Area	Avg	SD	Median	n
Flat	281.8	147.6	250.8	176
50nm	323.9	152.2	287.4	81
100nm	292.7	160.1	264.9	169
300nm	254.5	109.9	234.3	94
970nm	229.5	94.1	216.5	153

Figure 2.8 *Area of HGTFN cells after 18hours adhesion on flat, 50nm, 100nm, 300nm and 970nm deep x 2µm wide grooves.*

*Only the 970nm deep samples were significantly different from the flat surface. *=$p<0.01$. The shallow topography of the 50nm surface increased the spreading area of cells on this sample but this was not significant. However, individual parameters showed that the cells on the 970nm deep sample were not the only cells reacting to the topography.*

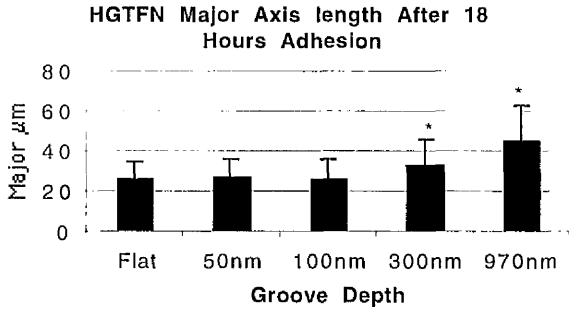

Maj Axis	Avg	SD	Median	n
Flat	25.8	9.5	24.0	176
50nm	27.3	8.7	25.7	81
100nm	26.2	9.5	24.9	169
300nm	33.4	12.4	30.9	94
970nm	44.7	18.1	43.4	153

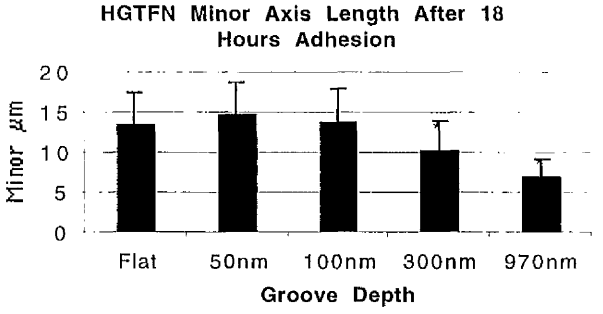

Min Axis	Avg	SD	Median	n
Flat	13.5	3.9	13.2	176
50nm	14.7	4.2	14.5	81
100nm	13.7	4.2	13.3	169
300nm	10.2	3.9	9.4	94
970nm	6.9	2.3	6.5	153

Figure2.9 *The axial lengths of HGTFN cells following 18 hours adhesion on 2µm wide grooves with various depths.*

*The major and minor axes only deviated from the flat surface cell parameters when the depth was >100nm. The 300nm and 970nm deep samples affected the endothelia by lengthening the major axis and narrowing the minor axis. This would account for the non-deviation from flat to 300nm deep in the area measurements. The significant narrowing of the cells counteracts the significant extension. *=$p<0.01$*

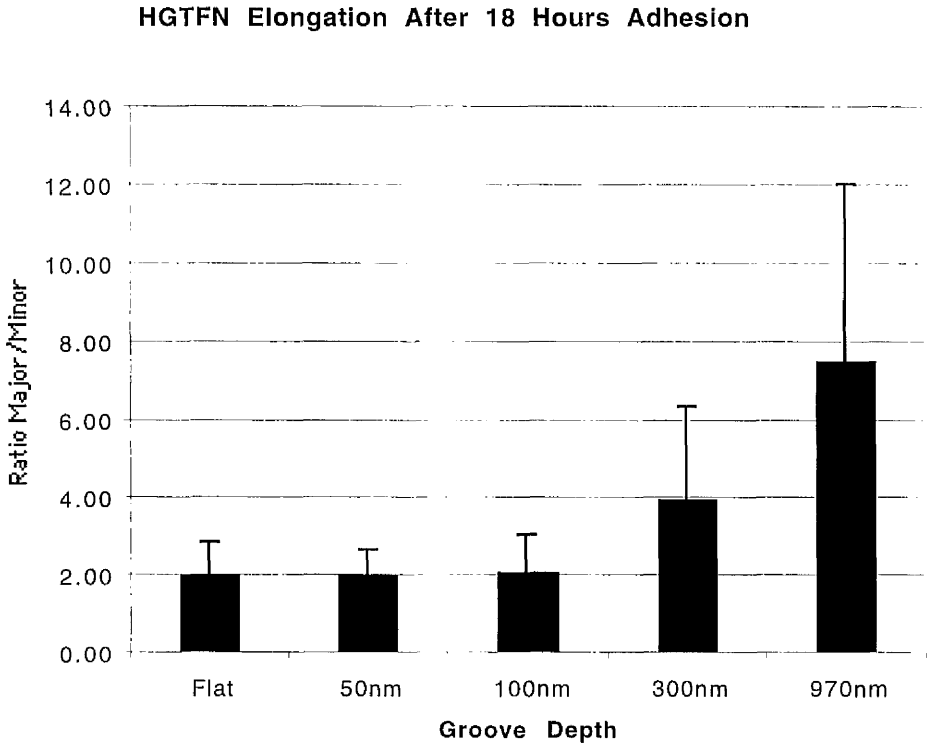

Figure 2.10. *HGTFN cell's major/minor axis ratios following 18 hours adhesion on varying groove depths.*

There was no difference in the flat, 50nm and 100nm samples when cultured until the cells are fully spread. The ratios of these three samples differ from the 3 hour sample. The three hour sample had a ratio of just over 1 but the 18 hour samples had a ratio of 2. There was a significant increase in the ratios of the 300nm (from around 2 to 4) and 970nm samples. The ratios doubled in the flat, 50nm, 100nm and 300nm samples (a doubling) but the 970nm deep sample extension has a ratio that more than doubles.

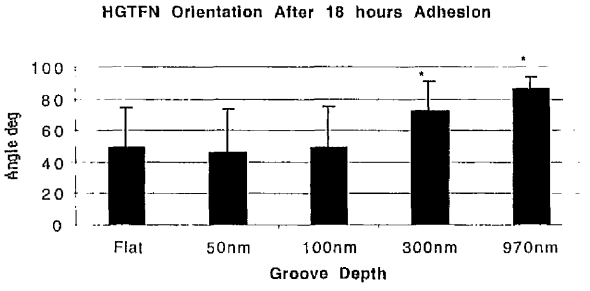

Angle	Avg	SD	Median	n
Flat	49.3	25.6	53.5	176
50nm	46.1	27.2	45.8	81
100nm	49.8	26.1	50.7	169
300nm	73.1	18.4	79.0	94
970nm	86.3	7.6	88	153

Figure 2.11 *The orientation of HGTFN cells on different groove depths following 18 hours adhesion.*

There was no significant difference between the 50nm or 100nm deep sample compared to the flat surface but when the cells are on 300nm or 970nm deep grooves the cells are oriented along the grooves. This orientation was depicted by the orientation being closer to 90 degrees (different from the three-hour sample because measurements were made on vertical grooves). The 970nm grooves orient the cells more than the 300nm samples

MDCK Cell Adhesion as Single Cells and Islets.

In the early nineties Peter Clark noticed that single cells of the epithelial cell line MDCK reacted differently to the cells in the middle of islets when cultured on grooves (Clark, Connolly et al. 1991). Single cells elongated along grooves of 100nm to 400nm in a similar fashion to previous studies of macrophages and fibroblasts (Wojciak-Stothard, Curtis et al. 1995; Wojciak-Stothard, Madeja et al. 1995). The extension along the grooves was depth dependent. The MDCK cells within multicellular islets showed directionality and stretch in the periphery of the islet. Those cells in the centre had no visible morphological difference to the cuboidal islets on a planer substrate. A complete MDCK cell monolayer showed no outward orientation. This result was confirmed primarily to characterise the cell morphology phenomenon before using these cells in video analysis on grooves. Figure 2.12 overleaf demonstrates the different morphologies of single cells and cells in multicellular islets.

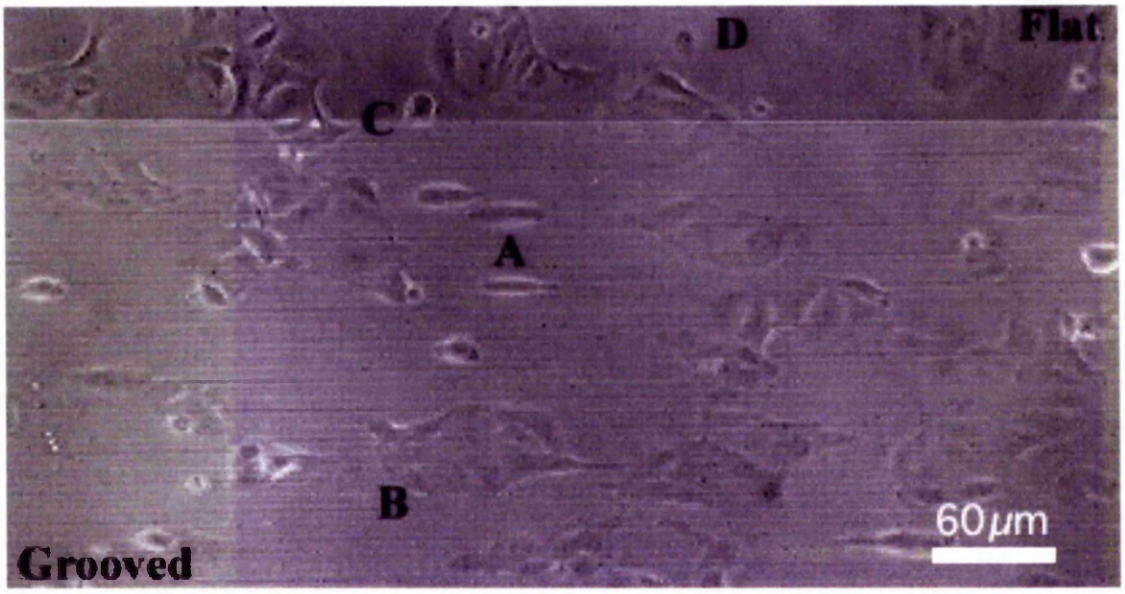

Figure 2.12 *MDCK cells grown on 2μm wide x 970nm deep parallel grooves for 30 hours.*

This video frame showed the different morphology of: A) elongated single cells; B) multicellular islets, with central cells not aligned to the topographical guidance; C) islets spanning the groove/flat area indicating a similar morphology on both types of surface; D) MDCK cells solely on the flat surface, where single cells did not elongate.

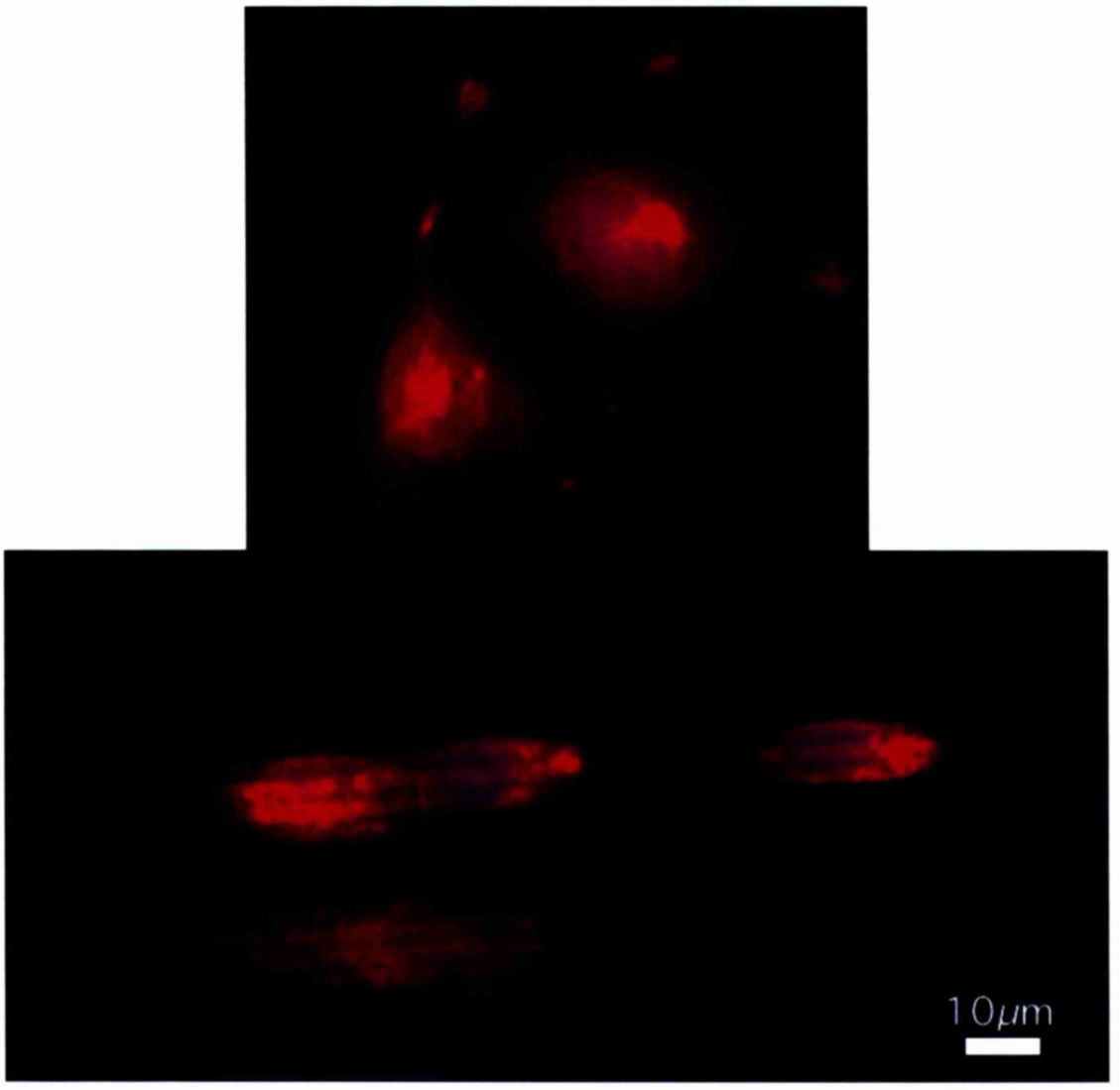

Figure 2.13 MDCK cell nuclear extension on flat and 2μm wide grooved surfaces.

MDCK cell membranes were stained with Texas Red and the Nucleus with Hoescht. There was slight elongation of the nucleus on the grooved surface (bottom). In general, there was minimal extension or alignment in the MDCK cell nucleus, whether on a flat surface (top) or on grooves. This was in contrast with HGTFN cells where the nucleus aligned to the groove and was elongated.

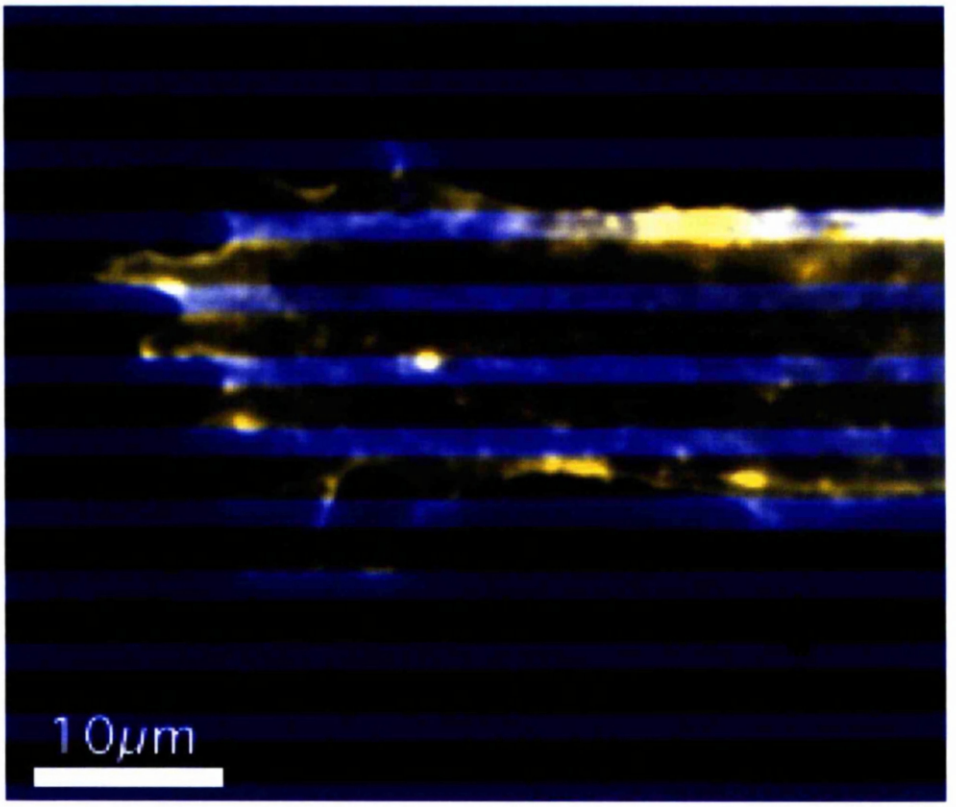

Figure 2.14 MDCK cell lamellipodia on 2μm wide x 970nm deep grooves.

MDCK cell membrane lamellipodia orient themselves along the groove edges. This morphology was only evident in single cells or those cells at the periphery of islets.

Discussion

The reaction of the endothelial cell line HGTFN, had not been fully characterised on parallel grooved topography. Guided movement had been shown to be along grooves (Curtis and Wilkinson 1997) but the reaction to various depths had not been determined. The aim of this set of preliminary experiments was to characterise the reaction of HGTFN cells to grooves with depths varying from 50nm to 970nm and also confirm the reaction of MDCK cells on these structures.

Morphology and Area

HGTFN endothelial cells reacted to grooves in a similar manner to reports of other cells. When adhesion time was limited to 3 hours, cell area on 100nm deep grooves and 300nm deep grooves was increased when compared to flat surfaces. Cell area on shallow 50nm grooves and 970nm grooves was unaffected but for different reasons. The cells morphology on the 50nm deep grooves were indistinguishable from the flat samples, but on 970nm deep grooves there was extensive elongation and alignment along the grooves. When cells were allowed to spread fully for 18 hours, there was a different result. The morphology of the cells on 50nm and 100nm deep grooves was subjectively indistinguishable from cells on a flat surface. The cell areas were also not significantly changed. On 300nm samples the cell area was increased after 3 hours adhesion compared to the flat samples. The cell area on 300nm deep grooves continued to rise up to 18 hours but the area of the flat samples increased more. This resulted in a net comparative decrease in cell area between the flat and 300nm sample

but this was not significant. Over three hours the area of cells on 970nm deep grooves was larger than the flat samples. The cell area continued to rise until 18 hours. After 18 hours, the flat sample area had overtaken the 970nm samples and resulted in a significantly lower are in the 970nm samples.

Orientation and Axes Dimensions

After 3 hours and 18 hours, the major axes orientation on the 300nm deep and 970nm deep samples were aligned along the grooves. On the 50nm and 100nm deep grooves the major axes had a distribution the same as on the flat surfaces. This suggested that HGTFN cells were only able to detect an orientation cue when the depth was greater than 100nm. They were also able to "sense" the depth difference between 300nm and 970nm deep. In figure 2.7 it was clear that the cell lamellipodia were not aligned on the 50nm and 100nm samples but they were either aligned along the groove edges or terminated on the groove edges on the 300nm and 970nm deep grooves. Not only were the major axis aligned on the deeper grooves, they were significantly larger after 3 hours and 18 hours. There was a significantly raised extension of the major axis of cells on 100nm deep grooves after three hours but this was due to increased spreading on the surface and not spreading along the grooves. This suggested that the cells were able to adhere on grooves quicker even though there was no orientation. There were distinct differences in the percentage increase of major and minor axes between 3 hours adhesion and 18 hours adhesion. This suggested that there was a similar spreading gradient over time for the major axes but the minor axes on 300nm and 970nm may be regulated differently.

Groove Depth	% Increase in Major Axis	% Increase in Minor Axis
Flat	55%	5%
50nm	64%	14%
100nm	46%	2%
300nm	58%	-16%
970nm	65%	-24%

Table 2.1 Percentage change in HGTFN cell axes length between 3 hours adhesion and 18 hours adhesion.

The percentage difference postulates that there may be two mechanisms of spreading on grooves. The major and minor axes seemed to spread at different rates. Table 2.1 suggests that the rate of width extension (minor axes) was depth dependent and decreased with increased depth. The major-axes spreading increased at the same rate between the two time periods, irrespective of the groove depth. If the dual spreading hypotheses is correct, the alignment of cells to grooves may be down to preferential alignment of one of the pathway progenitors. The spreading pathway hypotheses was tested in chapter 5 by blocking two pathways involved in adhesion signalling. Of course there is another parameter to be measured and that is the Z axis. If the width narrowing was due to tension generated in the major axis then this would result in the z-axis being reduced. However Chou (Chou, Firth et al 1995) found an increase in height of 1-1.5 times the height when cells were grown on V shaped grooves. Further work on the height of cells is required to assess this on square angled grooves and cells growing on the top of grooves.

MDCK Cell Morphology on Grooves

Previously the morphology of MDCK cells was characterised by Clarke on different parallel grooves (Clark, Connolly et al. 1991) and is covered further in the next chapter. However, the outcome was that single cells would elongate on grooves but the cells that formed cell-cell contacts would have reduced elongation. When these cell-cell contacts were part of multicellular islets (small groups of cells), the central cells had no apparent elongation or alignment to grooves but those on the periphery did have lamellipodia alignment. As the depth increased the orientation and alignment of single cells increased. Figures 2.12, 2.13 and 2.14 show the general morphology of MDCK cells on grooves. In HGTFN cells there was extension of the nucleus along grooves. In MDCK cells the nucleus extension was only evident in the elongated single cells but not in cell islets (Figure 2.13). This suggested that nuclear extension was only related to the overall cell morphology and not directly connected to the groove orientation. The difference in morphology of single cells and cell islets, led to an investigation of morphology related motility in chapter 3.

Chapter 3

Directed Movement.

Introduction

The migration of various cell types is altered on grooved topography compared with a flat surface (Brunette, Kenner et al. 1983, Clark, Connolly et al. 1991, Brunette 1987). On parallel grooved surfaces, cells will migrate bi-directionally along the groove; but on a flat surface they random walk. The speed of movement on grooves is also accelerated (Wojciak-Stothard, Madeja et al. 1995). Motility of varying cell types *in-vivo* plays a fundamental role in many biological systems, e.g. embryogenesis, angiogenesis, tumour invasion and wound repair (Holly, Larson et al. 2000). In nervous-system development, migration is essential for innervation of primary afferents into the dorsal spinal cord, for motoneurons to their musculoskeletal targets and for interneuron migration from the central canal to ventral laminae. Indeed Ahmed and Brown (Ahmed and Brown 1999) observed contact inhibition and increased motility of Schwann cells on fibronectin fibres and suggested that the motility could aid nerve repair. The fibronectin fibres had similar dimensions to the topography used in this chapter. Migration of cells is also required for other repair systems e.g. for wound closure. Here epithelial cell migration is required to re-establish the microbial barrier, and fibroblast migration within the wound is required for efficient tissue remodelling. Naturally, in development there are different types of cells adhering with one another resulting in more complex

tissue formation. This may affect the migratory properties, and should be noted, but this chapter was primarily concerned with the differences in motility of a homogeneous cell line on a microfabricated substratum. With regard to the mechanism of migration on a surface, it is established that actin polymerisation is the driving force behind extension of the leading lamellipodia in the direction of movement. This extension is aided by microtubules (Waterman-Storer, Worthylake et al. 1999) although they are not essential for lamellipodia formation (Ballestrem, Wehrle-Haller et al. 2000). On the other hand, microtubules are normally required for migration and tail retraction (Ballestrem, Wehrle-Haller et al. 2000), albeit not in the groove directed migration observed by Oakley and Brunette (Oakley and Brunette 1995; Oakley and Brunette 1995). In general however, there is not conclusive evidence for the mechanism by which cell bodies follow though Kaverina and colleagues (Kaverina, Krylyshkina et al. 2002) have shown microtubules to be the main element associated with tensile forces and stretch. It also remains unclear, which signalling mechanisms are involved for cell guidance and orientation along grooves.

This project's initial interest in MDCK cell movement on grooves, arose from the different elongation of multicellular-islets and single cells described by Clark et al (Clark, Connolly et al, 1991). Clark noticed that single MDCK cells elongated similarly to other cell types on parallel grooves. Those on the periphery of multicellular islets elongated parallel to grooves, whereas those cells inside islets did not have any outwardly apparent alignment. I wanted to determine if the single cells would have different movement patterns from the cell islets. Essentially, whether

there would be different movement of the two morphologically distinct groups. In addition, different cell types have different migration speeds on different topographies. Another consideration was whether there were differences in contact inhibition between migratory cells on grooves. This was not studied but it should be noted in any migration experiments. Directed movement would be useful, for example, in wound repair. Where a surface could selectively position certain cells in a desired location by utilising the differences in speeds of specific cell types on different groove dimensions. Furthermore, by altering the groove depths, one cell-type could be directed in preference to another, or grooves could be used in addition to chemotactic agents to direct movement into or out of the wound centre. This selective elongation-reaction to various depths is best seen when comparing the reaction of macrophages (Wojciak-Stothard, Curtis et al. 1996) and epithelia (Clark, Connolly et al. 1991). Generally cell migration on grooves is in the direction of the cell elongation, but not exclusive to elongated cells, since rounded cells will also move along grooves. There has been some debate that the migration of rounded cells is due to rolling for migration, or dependent on elongation. However, rounded recently passaged cells in an orthogonal flow, still have the ability to attach to grooves (J. Liddell, student honours project I assisted with) and therefore, still express adhesive proteins. Also, rounded cells forced to move on grooves following HGF treatment will immediately migrate along the groove. If migration was simple rolling, the initial movement would have no direction. The only observation to date on movement of rounded cells on grooved topography has been Hamilton's work on primary chondrocyte movement on 12.5μm wide grooves (Hamilton 2000). Another consideration, regarding observations of rounded cells, was whether they are actually

round. IRM studies by Hamilton (D. Hamilton, 2000) showed proximity to the substrate was not in the centre of the cell, suggesting primary chondrocytes may not be flattened but neither was the contact minimal. If a cell was totally round, then the substratum contact area would be in the centre of the cell. If a cell was domed then the contact area would be similar to the maximal diameter of the cell. Hamilton showed that the contact in chondrocytes on a substrate was somewhere in between the two scenarios. This suggested that migration of "rounded cells" was not simple rolling, but involved cell flattening. Cell lines are likely to be more flattened on the bottom and therefore, will have significant contact with the substratum. Whether this conveys an ability to migrate is open to debate, but neutrophils, which normally lack mature stress fibres and are rounded, also migrated along grooves and oligodendrocytes without actin fibres, extend extensively along parallel grooves (Webb, Clark et al. 1995). The mechanism for movement on grooves has not been determined so far but naturally the cytoskeleton is a target intermediary, considering the alignment of actin and microtubules on grooves. Microtubules however, are not necessarily required for directed movement providing actin stress fibres can form and compensate for their depolymerisation (Oakley and Brunette 1995) (Kaverina, Krylyshkina et al. 2000).

With regard to a potential use for directed epithelial cell migration, there are many instances where epithelial wounds do not close, or indeed close in parallel with other "undesirable" cells. The most obvious example being leg ulcers or bed-sores. This type of condition is common in diabetes, affecting 6% of the population. Normally in this long-term condition, re-epithelialisation occurs via migration over plasma-fibronectin/fibrin clots but this matrix also acts as a template for fibroblast and

macrophage migration. Previous studies relating to wound closure have concentrated on biochemical methods like collagenase stimulation of migration (Herman 1996) or modification of peptide fragments for enhanced taxis (Livant, Brabec et al. 2000). Some clinical work also suggested that a fibrous mesh was beneficial. Hollander used modified hyaluronan fleece with reduced degradation properties (also without aligned fibres) to heal leg sores in a patient that refused surgery (Hollander, Schmandra et al. 2000). However, in these situations, treatment may require optimisation of many parameters in each case study. Therefore, using a homogenous template, with growth-factor mobility inducement, may be a more cost-effective scenario, whereby the increased migration speed and closing of the wound, would reduce the potential for infection.

Summary of Experiments

With regard to topographical effect on migration, the original intention was to look at differences in motility of epithelial cells and endothelial cells on varying topography. The hypotheses being that different cell morphologies on different topography, would correlate with differences in migration. Another consideration would be whether the different depths would influence migration speeds.

However, when surveying the minimal motility of the morphologically distinct, single and multicellular MDCK epithelial cells in the initial experiments, it was more interesting for this study to pursue a forced migration approach using growth factors. Interestingly the cell type (MDCK cells) and the method of motility-induction (HGF), are relevant for liver repair and indeed have been used widely as an epithelial model

(Dugina, Alexandrova et al. 1995; Royal and Park 1995; Royal, Fournier et al. 1996; Tsukamoto and Nigam 1999; Yanagihara, Miura et al. 2001).

In addition to the initial investigation into facilitated movement, the possibility of unidirectional movement was also assessed. The surface used had parallel major grooves with sub-gradients in the troughs with shallow slopes in one direction and steeper slopes in the other. The natural hypothesis here, was that cells would prefer to encounter a gentle surface rather than climb up a steeper slope, but that was not necessarily the feature "sensed" by cells. For this series of experiments HGTFN endothelial cells were used in preference to MDCK cells (though not exclusively) to eliminate the difference in morphology observed between single cells and islets. MDCK cells were used to determine if they would move in one direction. The hypotheses being that if MDCK cells had a weak bi-directional migration force in both directions that cancelled each other out, a surface that may produce a net unidirectional force may move them in one direction. Obviously, if a surface could confer unidirectional movement, it would be beneficial to wound repair. If used in parallel with cell specific adhesion (or inhibition of adhesion), individual cell types could be guided to the site of repair or indeed forced to migrate away from the repair site. Directed movement could be used in many clinical situations like nerve regeneration (Ahmed and Brown 1999; Dubey, Letourneau et al. 1999). Many researchers are striving for a surface that will preferentially direct cells in on direction. Such surfaces have varied from horizontal Christmas tree shapes, to narrowing grooves and even galvanotaxis chambers, which direct cells to the cathode (Sulik, Soong et al. 1992).

Materials and Methods

Cell Culture

MDCK cells were passaged as described in chapter 2. Following resuspension the cells were added in 300µl aliquots onto the surface and allowed to adhere for 1 hour in a moist chamber. The cell density in the droplet was dependent on whether the cells were to be observed as single cells (20,000/ml) or as clumps of cells adhering while in contact with each other (80,000/ml).

Hepatocyte Growth Factor

HGF was used at a concentration of 300 units/ml.

Video Capture and Analysis

Images for MDCK cell movement video were captured at 4x and 10x magnification (Zeiss Axiovert 20 microscope) by CCD camera in SVHS format on a Panasonic time-lapse video recorder. The individual frames were captured on a Macintosh PowerPC Computer fitted with digitising card using NIH Image software. Images were converted to tiff stacks and subsequently, QuickTime movies.

Directed Movement Structure

The surface used for directed movement was designed and manufactured by David Baxter, a final year project student (Electronics and Electrical Engineering, University of Glasgow). The surface was made using anisotropic etch techniques to generate a surface with different slopes in the bottom of parallel grooves.